pubs.acs.org/acschemicalbiology

Article

Transcriptomics-Driven Discovery of New Meroterpenoid Rhynchospenes Involved in the Virulence of the Barley Pathogen *Rhynchosporium commune*

Reynaldi Darma,[¶] Zhuo Shang,*[,¶] Joe Bracegirdle, Stephen Moggach, Megan C. McDonald, Andrew M. Piggott, Peter S. Solomon,* and Yit-Heng Chooi*

Cite This: *ACS Chem. Biol.* 2025, 20, 421−431

Read Online

ACCESS | Metrics & More | Article Recommendations | Supporting Information

ABSTRACT: *Rhynchosporium commune*, the causal agent of barley scald disease, poses a major threat to global barley production. Despite its significant impact, the molecular mechanisms underlying *R. commune*'s infection process remain largely unexplored. To address this, we analyzed the differential gene expression data of *R. commune* WAI453 cultivated under both *in planta* and *in vitro* conditions, aiming to identify secondary metabolite biosynthetic gene clusters that are potentially involved in the pathogenicity of *R. commune*. Our analysis revealed increased expression of a polyketide-terpene gene cluster (the *rhy* cluster), containing a specific myeloblastosis (MYB)-type transcription factor gene *rhyM*, during *in planta* growth. Overexpression of *rhyM* in an axenic culture activated the expression of the *rhy* cluster, resulting in the production of a series of new meroterpenoid metabolites, which we named rhynchospenes A−E. Their structures were elucidated through a combination of spectroscopic methods and single crystal X-ray diffraction analysis. Infiltration of rhynchospenes into barley leaves resulted in strong necrosis, with rhynchospene B demonstrating the highest phytotoxicity and causing necrosis at a minimum concentration of 50 ppm. Silencing *rhyM* in *R. commune* WAI453 confirmed the role of rhynchospenes as virulence factors in barley disease. The resulting mutant showed significantly reduced expression of the *rhy* cluster *in planta* compared to the wild-type strain and decreased virulence in seedling pathogenicity assays on barley. The characterization of the *rhy* cluster and rhynchospenes provided insights into the role of secondary metabolites in *R. commune* virulence and barley scald disease development. The study also highlights the potential use of MYB-type transcription factor overexpression in uncovering cryptic SMs involved in pathogenicity and host adaptations.

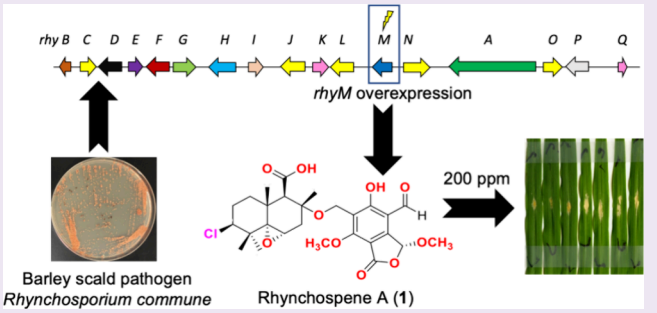

Downloaded via AUSTRALIAN NATL UNIV on May 1, 2025 at 03:07:49 (UTC).
See https://pubs.acs.org/sharingguidelines for options on how to legitimately share published articles.

INTRODUCTION

Rhynchosporium commune is a fungal pathogen responsible for barley scald disease—a destructive global barley disease causing up to 45% yield loss in high humidity production areas.[1] Despite heavy fungicide treatment, financial losses as high as £7.2 million have been documented in the UK.[2] *R. commune*, which was previously known as *Rhynchosporium secalis* (Oud.) J.J. Davis,[3,4] is considered a hemibiotroph due to its long asymptomatic phase in infected leaves prior to inducing cell death.[5] Barley scald disease also reduces grain quality leading to the substantial losses attributed to the disease.[5−7]

Secondary metabolites (SMs) play a crucial role in the pathogenicity of fungal phytopathogens. For instance, wheat pathogen *Parastagonospora nodorum*, which causes septoria nodorum blotch, secretes several different phytotoxic SMs during infection. These include elsinochrome C, which induces necrosis in wheat leaves,[8] as well as phomacin D and alternapyrone F, which inhibit seed germination.[9,10] SMs produced by *R. commune* were first reported 50 years ago, when a phytotoxic elicitor molecule was discovered in the filtrate from cultures grown in oat media.[11] The compound was subsequently identified as a cellobioside of 1,2-propanediol, which induces necrosis on some lines of barley, rye, wheat, oats, and other non-native hosts of *R. commune*.[12] Another phytotoxic SM, (+)-orthosporin, has been characterized from *Rhynchosporium orthosporum*, a sister species of *R. commune* that infects orchard grass.[13,14] This compound has also been isolated from two other nonrelated fungi, *Aspergillus ochraceus* and *Drechslera siccans*.[15,16] (+)-Orthosporin has the ability to inhibit the root growth of orchard grass and lettuce.

Received: October 25, 2024
Revised: January 15, 2025
Accepted: January 27, 2025
Published: February 12, 2025

© 2025 American Chemical Society

https://doi.org/10.1021/acschembio.4c00731
ACS Chem. Biol. 2025, 20, 421−431

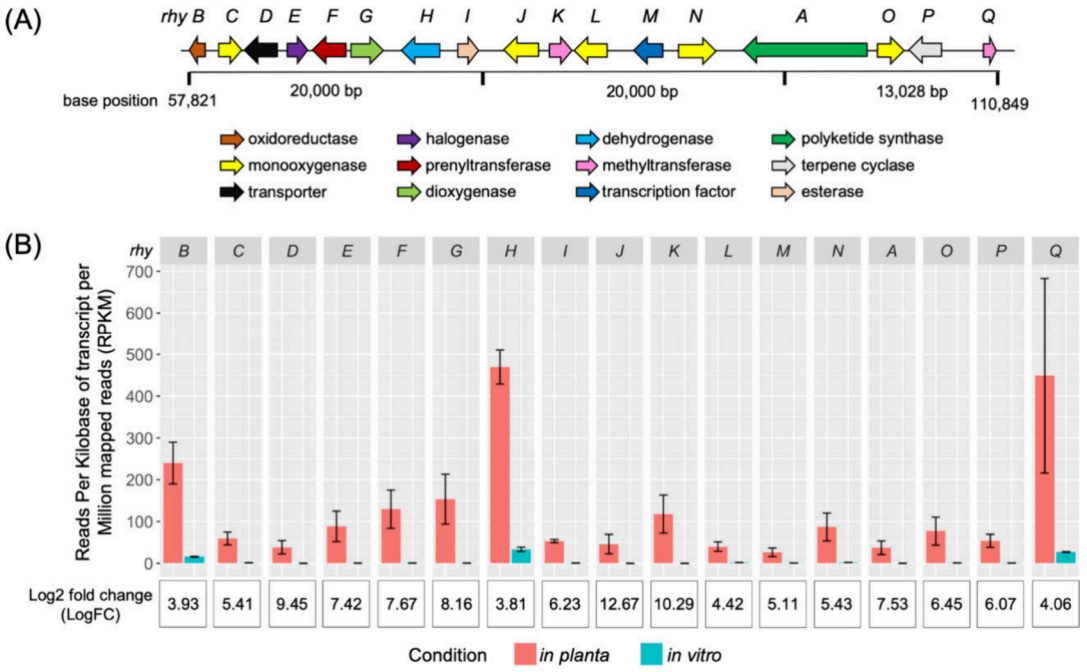

Figure 1. Gene organization of the *rhy* BGC and expression level of each gene within the cluster during *in planta* growth. (A) The *rhy* biosynthetic gene cluster contains 17 genes and spans 53 kb from base position 57821 to 110849 on contig 9 of the *R. commune* WAI453 genome assembly. (B) All 17 genes of the *rhy* cluster were upregulated during *in planta* growth, but were expressed at low levels or not expressed during *in vitro* growth. RNA was isolated from leaves of barley 8-days postinfection (dpi) with *R. commune* WAI453 (*in planta*) and 8-day old *in vitro* culture.

To our knowledge, no other characterized SMs have been reported from *R. commune*.

The majority of fungal SMs are encoded by groups of colocalized genes, known as biosynthetic gene clusters (BGCs), which typically include core biosynthetic genes encoding enzymes responsible for the synthesis of the backbone of metabolites, as well as genes involved in tailoring of the metabolites. Fungal SMs exhibit remarkable diversity, with major classes including polyketides, nonribosomal peptides, terpenes, cyclodipeptides, and ribosomally synthesized and post-translationally modified peptides (RiPPs). These SM classes are categorized based on the core biosynthetic enzymes that shape SM backbones.[17,18] Recent genome sequencing studies have revealed that species within the genus *Rhynchosporium* are rich in SM BGCs,[19] among which 14 polyketide synthases (PKSs), eight nonribosomal peptide synthetases (NRPSs), three dimethylallyl tryptophan synthases (DMATSs), and one terpene synthase/cyclase (TC) were predicted as the core enzyme of BGCs.[19] However, in contrast to the large number of BGCs, few SMs from *R. commune* have been reported.[11,12] This suggests that the SM repertoire of *R. commune* is largely unexplored, and there maybe virulence-related SMs to be uncovered. Although both the cellobioside of 1,2-propanediol and (+)-orthosporin have been characterized, they have not been linked with any BGCs from *Rhynchosporium* species. Furthermore, many BGCs in fungi are not expressed or are expressed at low levels under laboratory axenic conditions. These so-called "cryptic" SMs might only be induced in response to environmental stimuli, such as during interactions with host organisms.[20]

To uncover cryptic virulence-related SMs in *R. commune*, we employed a chemical ecogenomics strategy.[10,20] This approach identified an upregulated BGC (*rhy*) during *in planta* growth of *R. commune* WAI453. Overexpression of the *rhy* cluster-specific transcription factor RhyM activated expression of the *rhy* cluster in an axenic culture, leading to the production of five new meroterpenoid metabolites, which we named rhynchospenes A–E (**1**–**5**). Furthermore, we validated the role of rhynchospenes as virulence factors in barley scald disease through barley leaf infiltration assays and RNAi-mediated silencing of *rhyM*. These findings expand our understanding of the biosynthetic capabilities of the barley scald pathogen *R. commune* and shed new light on its mechanisms of infection and disease induction in barley.

RESULTS AND DISCUSSION

Biosynthetic Gene Cluster Prediction and Transcriptomic Analysis of *R. commune*. BGCs responsible for SM biosynthesis in the *R. commune* WAI453 genome were first predicted using antibiotics & Secondary Metabolite Analysis Shell (antiSMASH).[21] The analyses identified 53 putative SM BGCs, including 11 PKS clusters, 15 NRPS clusters, three PKS-NRPS hybrid clusters, 15 RiPP clusters, eight terpene clusters, and one PKS-terpene hybrid cluster. Next, we analyzed an existing *R. commune* WAI453 transcriptomic data set[22] to identify BGCs upregulated during *in planta* growth. Differential gene expression analysis revealed seven putative BGCs that were upregulated specifically during *in planta* growth, while being inactive or lowly expressed during axenic growth (Table S1, Data File S1). The significant upregulation of these BGCs during *in planta* growth suggested that they may play a role in facilitating the development of barley scald disease.

The *rhy* Biosynthetic Gene Cluster Is Highly Upregulated during *in Planta* Growth. One BGC that was highly expressed during *in planta* growth of *R. commune* WAI453 is the PKS-terpene hybrid cluster located on contig 9 of the WAI453 genome assembly (GenBank assembly: GCA_046529785.1). This cluster, subsequently named the *rhy* cluster (Figure 1A), was predicted by antiSMASH to

https://doi.org/10.1021/acschembio.4c00731
ACS Chem. Biol. 2025, 20, 421–431

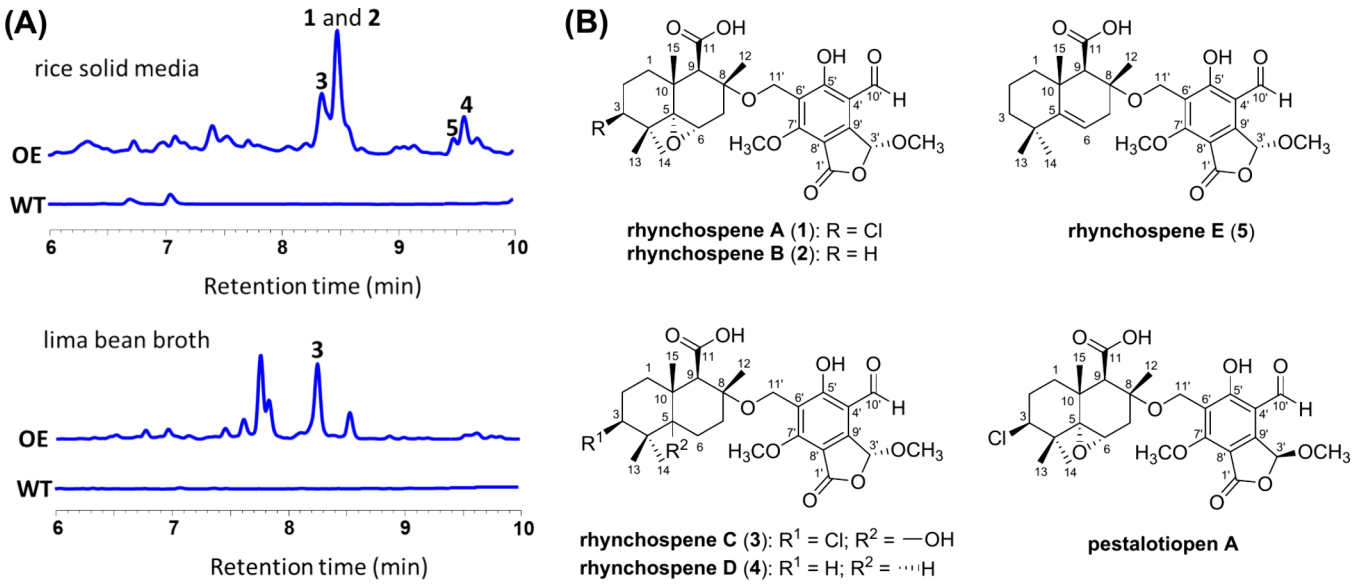

Figure 2. Overexpression of transcription regulator RhyM led to the production of rhynchospenes by *R. commune* WAI453 in axenic culture. (A) HPLC traces (220 nm) of the EtOAc extracts of wild-type *R. commune* WAI453 and the *rhyM*-OE mutant were cultivated in rice solid media and lima bean broth. (B) Chemical structures of rhynchospene A–E (**1**–**5**), along with the previously reported pestalotiopen A.

contain diagnostic genes for PKS, fungal-RiPP-like, and indole cluster families (Table S1). This cluster contains many genes that were upregulated with a Log2 Fold Change (LogFC) > 3 during *in planta* growth, including *WAI453_008914*, which encodes a PKS megasynthase (designated as *rhyA*; LogFC = 7.53) (Figure 1B and Data File S1). The expression of *rhyA* peaked during the onset of necrotrophy [6–8-days post-infection (dpi)], with lower expression observed during both the early and the later stages of infection (Figure S1). Subsequent analysis of the expression of genes flanking *rhyA* revealed that three upstream genes (*rhyO*–*rhyQ*) and 13 downstream genes (*rhyB*–*rhyN*) were substantially upregulated during *in planta* growth, while displaying low expression levels in axenic culture (Figure 1B). These results suggested that the *rhy* cluster contains 17 genes (*rhyA*–*rhyQ*) spanning approximately 53 kb in the *R. commune* WAI453 genome (Figure 1A). The gene *WAI453_008900* and genes *WAI453_008918*–*WAI453_008924* adjacent to the *rhy* cluster are not coregulated (Data File S1) and are therefore not considered as part of the *rhy* cluster.

To predict the type of SMs encoded by the *rhy* BGC, an in-depth analysis of each gene within the cluster, and the function of its corresponding enzyme, was conducted using BLASTP. Results indicated that the *rhy* cluster encodes a PKS (RhyA), five cytochrome P450 monooxygenases (RhyC, RhyJ, RhyL, RhyN, and RhyO), two methyltransferases (RhyK and RhyQ), an oxidoreductase (RhyB), a dioxygenase (RhyG), a dehydrogenase (RhyH), an esterase (RhyI), an aromatic prenyltransferase (RhyF), a DUF3328 protein (RhyE), a myeloblastosis (MYB) transcription factor (RhyM), a transporter (RhyD) and a hypothetical protein with no putative conserved domains (RhyP) (Figure 1A and Table S2). Domain analysis of RhyA using synthaser,[23] which is based on the NCBI Conserved Domain Search (CD-Search),[24] revealed six domains, including ketosynthase (KS), acyltransferase (AT), product template (PT), acyl carrier protein (ACP), methyltransferase (MT), and thioesterase (TE), indicating RhyA is a nonreducing PKS (NR-PKS) (Figure S2A). Given NR-PKSs often contain a starter acyltransferase (SAT) domain at the N-terminus and there is a ∼ 350 amino acid N-terminal region with no predicted conserved domain, additional analyses of the RhyA N-terminus were conducted using Alphafold[25] followed by Foldseek[26] to search for similar structural folds, as well as homology modeling with Phyre2.[27] The results revealed that the N-terminus of RhyA exhibits structural similarity to the SAT domain of CazM involved in chaetoviridin biosynthesis (PDB ID: 4RPM).[28] The presence of conserved active site residues suggests that RhyA likely possesses an active SAT domain (Figures S2B–S2D). The amino acid sequence of RhyA is similar to those of other PKS proteins involved in meroterpenoid biosynthesis. Specifically, RhyA shares 58.8% similarity with MfmB (from *Annulohypoxylon moriforme* CBS 123579) involved in the biosynthesis of 11′-*O*-desmethylfendlerol A/B,[29] 42.4% similarity with AdrD (from *Penicillium roqueforti*) involved in andrastin A biosynthesis,[30,31] 50.0% similarity with AndM (from *Colletotrichum higginsianum*) involved in anditomin biosynthesis,[32,33] and 42.2% similarity with MpaC (from *Penicillium roqueforti*) involved in mycophenolic acid biosynthesis.[34] However, RhyA shares only 30.2% similarity with AscC (from *Acremonium egyptiacum*), which is involved in the biosynthesis of the orsellinic acid-derived meroterpenoid ascochlorin,[35] and only 29% similarity with Mld15 (from the basidiomycete *Armillaria ostoyae*) in the biosynthesis of melleolide-type meroterpenoids.[36] Nevertheless, the presence of an aromatic prenyltransferase (RhyF) within the *rhy* cluster strongly suggested that BGC most likely encodes polyketide-terpene hybrid SMs, a predominant member of the meroterpenoid family.

Overexpression of the Cluster-Specific Transcription Factor RhyM for SM Production. As transcription of the *rhy* cluster occurs exclusively during *in planta* growth, characterization of the SM products encoded by the cluster through *in situ* cultivation is challenging. The infected leaf extracts contain a mixture of fungal and plant metabolites, and the overall yields of target SMs are too low for structure elucidation. Overexpression of cluster-specific transcription factors has been previously employed to uncover SMs from cryptic fungal BGCs.[9,37] Therefore, we aimed to activate the expression of

https://doi.org/10.1021/acschembio.4c00731
ACS Chem. Biol. 2025, 20, 421–431

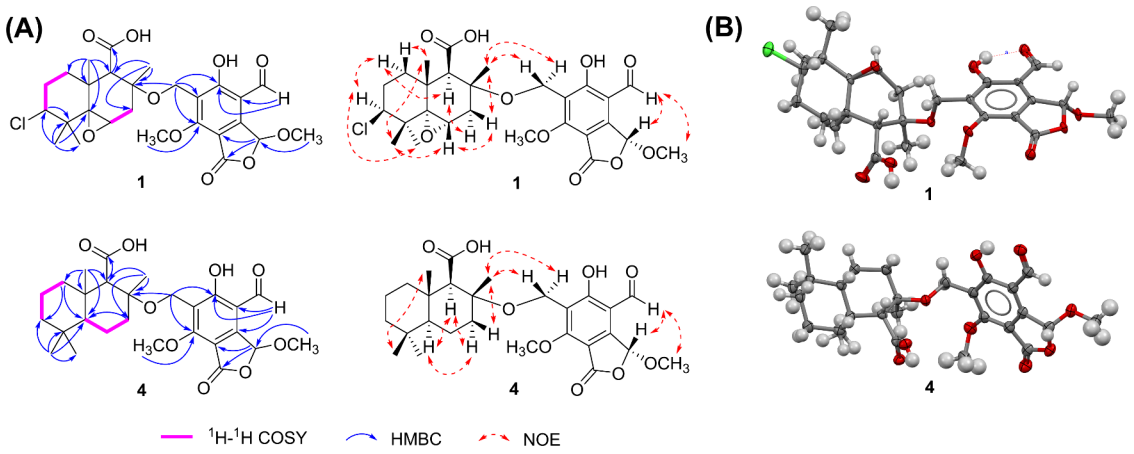

Figure 3. Structure elucidation of rhynchospenes A (**1**) and D (**4**). (A) Selected 2D NMR correlations of **1** and **4**. (B) Single crystal X-ray diffraction analyses of **1** and **4**. Displacement ellipsoids for non-H atoms are drawn at the 50% probability. Atoms are colored: C l −green, O − red, C − gray, H − white. Intramolecular H-bonds are represented by a dashed red line. Crystallographic data were deposited in the Cambridge Structural Database (CCDC 2379049).

the *rhy* cluster in axenic culture by overexpressing the predicted MYB transcription factor, RhyM. Although MYB-class transcription factors have rarely been implicated in SM pathway regulation, we hypothesized that RhyM could act as a pathway-specific transcription factor for the *rhy* cluster based on the colocalization of *rhyM* with the cluster. To overexpress *rhyM*, an overexpression construct (*rhyM*-OE) was introduced ectopically into the genome of *R. commune* WAI453 using *Agrobacterium tumefaciens*-mediated transformation (ATMT). Quantitative reverse transcription PCR (qRT-PCR) analysis confirmed the expression of *rhyM* in the *R. commune rhyM*-OE mutant, whereas the gene was not expressed in the axenic culture of the wild-type strain (Figure S3). Subsequent analysis of other genes within the *rhy* BGC in *R. commune rhyM*-OE confirmed the upregulation of the PKS gene *rhyA* and the prenyltransferase gene *rhyF*, indicating that the transcription factor RhyM exerts regulatory control over the other genes in the *rhy* cluster (Figure S3). Having observed the activation of the *rhy* cluster in the RhyM overexpression mutant, we next sought to identify the product of the *rhy* cluster from an axenic culture of the *R. commune rhyM*-OE mutant. HPLC analysis of the mutant strain cultivated in lima bean broth and on rice solid media revealed a series of chromatographic peaks that were absent in the culture of the wild-type *R. commune* WAI453 strain (Figure 2A), suggesting the production of SMs related to the *rhy* cluster.

Our study demonstrated that RhyM, the MYB-type transcription factor in the *rhy* cluster, positively regulates the expression of other genes within the cluster. It is noted that the most prevalent type of transcription factor in fungi is the $Zn(II)_2Cys_6$ class, accounting for approximately 90% of regulators within fungal PKS gene clusters.[38,39] Conversely, MYB-type transcription factors are rare among fungi, although they are abundant in plant genomes.[40,41] MYB-type transcription factors comprise less than 10% of the total types of transcription factors in various Ascomycetes and Basidiomycetes with different lifestyles.[40] Although MYB-type transcription factors are commonly distributed across nonspecific loci throughout different chromosomes in fungal genomes,[42] a limited number are found within BGCs.[43] For example, *mtf1* from the hemibiotrophic Basidiomycete *Ustilago maydis*, which is part of a PKS gene cluster involved in pigment biosynthesis, encodes a MYB-family transcription factor that positively regulates the expression of 12 genes within the cluster.[43] Only a limited number of fungal MYB-type transcription factors have been characterized to date, with some shown to be involved in regulation of traits important for environmental adaptations.[44,45] For example, MoMyb13 from *Magnaporthe oryzae* is involved in multiple biological aspects including growth, conidiation, stress resistance, and pathogenicity,[44] while MYB36 from the biocontrol fungus *Trichoderma asperellum* is important for the protection of its poplar host against the pathogen *Alternaria alternata*.[45] Given the involvement of MYB-type transcription factors of other fungi in environmental adaptations, such as pathogenicity and mutualism, it is tantalizing to speculate that the SMs encoded by *rhy* cluster regulated by MYB-type RhyM could be important for *R. commune* adaptations, such as pathogenicity.

Scaled-Up Cultivation and Structure Elucidation of Rhynchospenes A−E (1−5). To characterize the SMs expressed by the *rhy* cluster, the *R. commune rhyM*-OE strain was cultivated on rice solid media for 60 days and in lima bean broth at 20 °C for 8 days for large-scale production. Ethyl acetate extraction of the rice media culture, followed by preparative HPLC, led to the isolation of compounds **1**−**5** with almost identical UV−vis spectra (Figures 2B and S4), suggesting that they are biosynthetically related. The structures of **1**−**5** were elucidated by using high-resolution mass spectrometry (HRMS), nuclear magnetic resonance spectroscopy (NMR), electronic circular dichroism spectroscopy (ECD), and single-crystal X-ray diffraction analysis, as described below. In contrast, the yield of extract from lima bean broth culture was too low to isolate any metabolites for NMR analysis. However, LC-MS and HR-MS analyses of the extract revealed two additional peaks at retention times of 7.7 and 7.8 min, with molecular formulas of $C_{26}H_{34}O_9$ and $C_{26}H_{36}O_9$, respectively (Figures 2A and S5). These peaks exhibited UV−vis spectra distinct from those of compounds **1**−**5** (Figure S4), suggesting they are either structurally unrelated or have significant modifications to the chromophore.

Rhynchospene A (**1**) was isolated as a pale-yellow oil. HRESI(−)MS analysis of **1** returned deprotonated and formate-adduct ions indicative of a molecular formula

https://doi.org/10.1021/acschembio.4c00731
ACS Chem. Biol. 2025, 20, 421−431

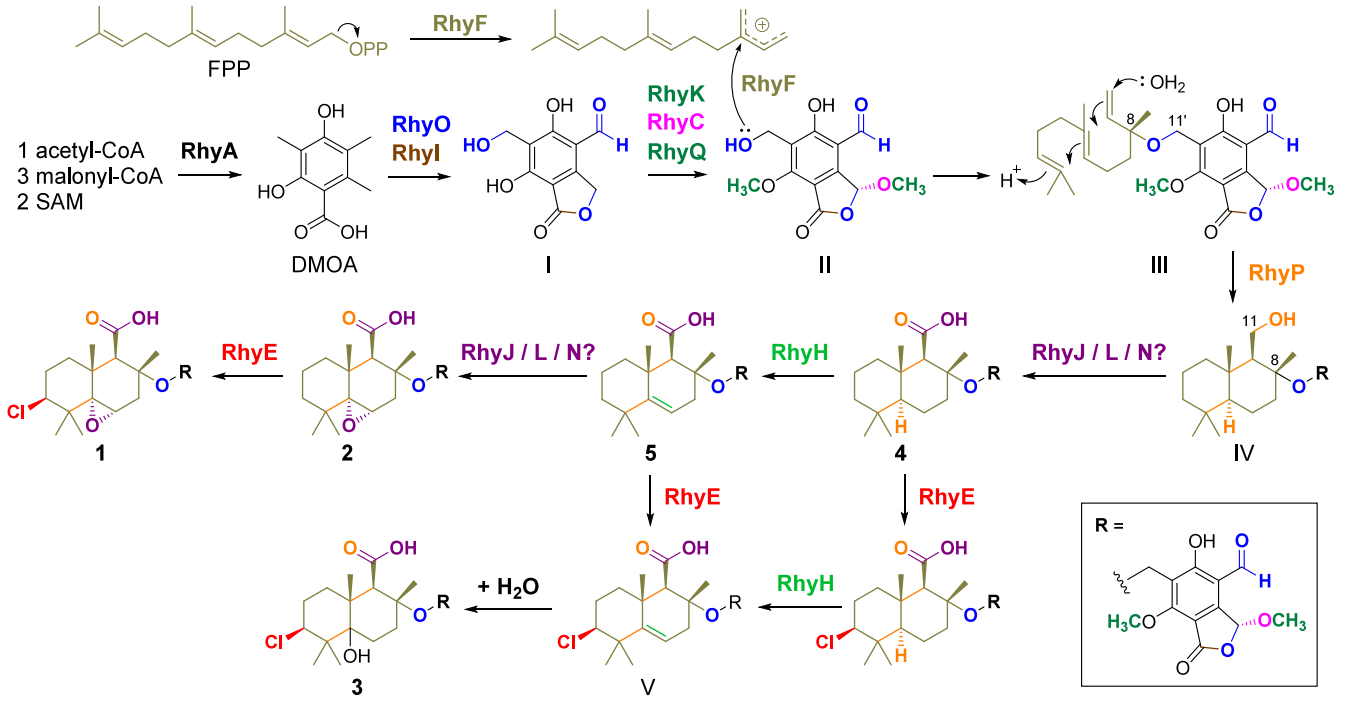

Figure 4. Proposed biosynthetic pathway to rhynchospenes A–E (**1**–**5**). A more detailed biosynthetic pathway to the rhynchospenes is shown in Figure S11.

$C_{27}H_{33}O_{10}Cl$, requiring 11 double bond equivalents (DBEs) (Figure S7). Detailed 1D and 2D NMR analysis ($CDCl_3$) permitted the identification of a bicyclic decalin sesquiterpene (drimane) substructure (C-1 to C-15) connected to 3′-*O*-methyl-11′-hydroxycyclopaldic acid (C-1′ to C-11′) (Tables S3 and S6, Figures 3A and S15–S20). The presence of an aldehyde group at C-4′ was confirmed by the presence of HMBC correlations from H-10′ to C-4′ and C-5′. Furthermore, the connectivity between the drimane and cyclopaldic acid substructures was established as being through an ether bond, as evidenced by the HMBC correlation from H_2-11′ to C-8 (Figure 3A). Comparison of the NMR data for **1** with those for pestalotiopen A, a natural product containing a sesquiterpene-cyclopaldic acid hybrid isolated from an endophytic fungus *Pestalotiopsis* sp.,[46] revealed almost identical NMR, indicating that **1** shares the same planar structure as pestalotiopen A. The absolute configuration of **1** was unambiguously assigned as (3*S*, 5*S*, 6*S*, 8*R*, 9*R*, 10*R*, 3′*R*) by single crystal X-ray diffraction analysis (Figures 3B and S45, Table S11), revealing that **1** is the 3′-epimer of pestalotiopen A. Comparison of the experimental ECD spectra of **1** and pestalotiopen A revealed a strong negative Cotton effect at 250 nm in both compounds (Figure S6). However, pestalotiopen A exhibited an additional negative Cotton effect at 297 nm,[46] which was absent in **1**. Given the absolute configuration of pestalotiopen A was only tentatively assigned based on optical rotatory dispersion (ORD) and ECD DFT calculations, our single crystal X-ray diffraction analysis provides a definitive determination of the absolute configuration of this class of sesquiterpene-cyclopaldic acid hybrid meroterpenes.

With the unequivocal establishment of the structure, including the absolute configuration of **1**, we proceeded to assign the structures of **2**–**5** through a comparative analysis of HRMS, NMR, and ECD data (Tables S3 and S7–S10, Figures S6, S7 and S21–S44). Specifically, rhynchospene B (**2**) was identified as a dechlorinated analogue of **1** as evidenced from the molecular formula $C_{27}H_{34}O_{10}$ and the replacement of NMR resonances for a H-3 methine (δ_H 3.94, δ_C 68.5) with those for a H_2-3 methylene (δ_H 1.36, δ_C 38.1) (Figure S7, Table S3). The comparable Cotton effects in the ECD spectra of **1** and **2** [λ_{max} ($\Delta\varepsilon$): 226 (+7.6), 250 (−14.4), 307 (+0.4) for **1**; λ_{max} ($\Delta\varepsilon$): 226 (+9.3), 250 (−17.9), 305 (+0.3) for **2**] suggested that **1** and **2** share the same absolute configuration, particularly at C-3′ (Figure S6). Rhynchospene C (**3**), with the molecular formula $C_{27}H_{35}O_{10}Cl$, exhibited a significant alteration with a methylene group (δ_H 1.75/1.94, δ_C 26.7) at C-6 instead of the oxymethine group (δ_H 3.25, δ_C 53.7) present in **1** (Figure S7, Table S3). This suggests that **3** contains a C-5 hydroxy instead of a C5/C6-epoxide in **1**. Rhynchospene D (**4**), identified as the C-5 and C-6 deoxygenated product of **2**, exhibited a shielding effect at C-5 ($\Delta\delta_{C\text{-}5}$ − 10.6) and C-6 ($\Delta\delta_{C\text{-}6}$ − 33.9) (Table S3). Single crystal X-ray diffraction analysis confirmed the absolute configuration of **4** to be the same as that of **1**, with C-5 having an *S* configuration (Figures 3B and S46, Table S12). Rhynchospene E (**5**) is a C-5/C-6 dehydrogenated analogue of **4**, characterized by the presence of resonances indicative of an olefinic bond ($\delta_{C\text{-}5}$ 150.0, $\delta_{C\text{-}6}$ 117.5) (Table S3). This was confirmed by HMBC correlations from H-7 to C-6 and from H-13/H-14 to C-5, along with a COSY correlation between H-6 and H-7 (Figure S8). Based on the NOE correlations, comparable Cotton effects, and biosynthetic consideration (Figures S6 and S9), the absolute configuration of **5** was deduced to be the same as **1**–**4**.

Proposed Biosynthesis of Rhynchospenes. It is curious that *rhy* cluster was predicted to be a "PKS-fungal-RiPP-like/indole hybrid" BGC by antiSMASH when its upregulation led to the production of a series of polyketide-terpene meroterpenoids. This is likely due to the detection of the *rhyE* gene encoding a DUF3328 protein, which belongs to a

https://doi.org/10.1021/acschembio.4c00731
ACS Chem. Biol. 2025, 20, 421−431

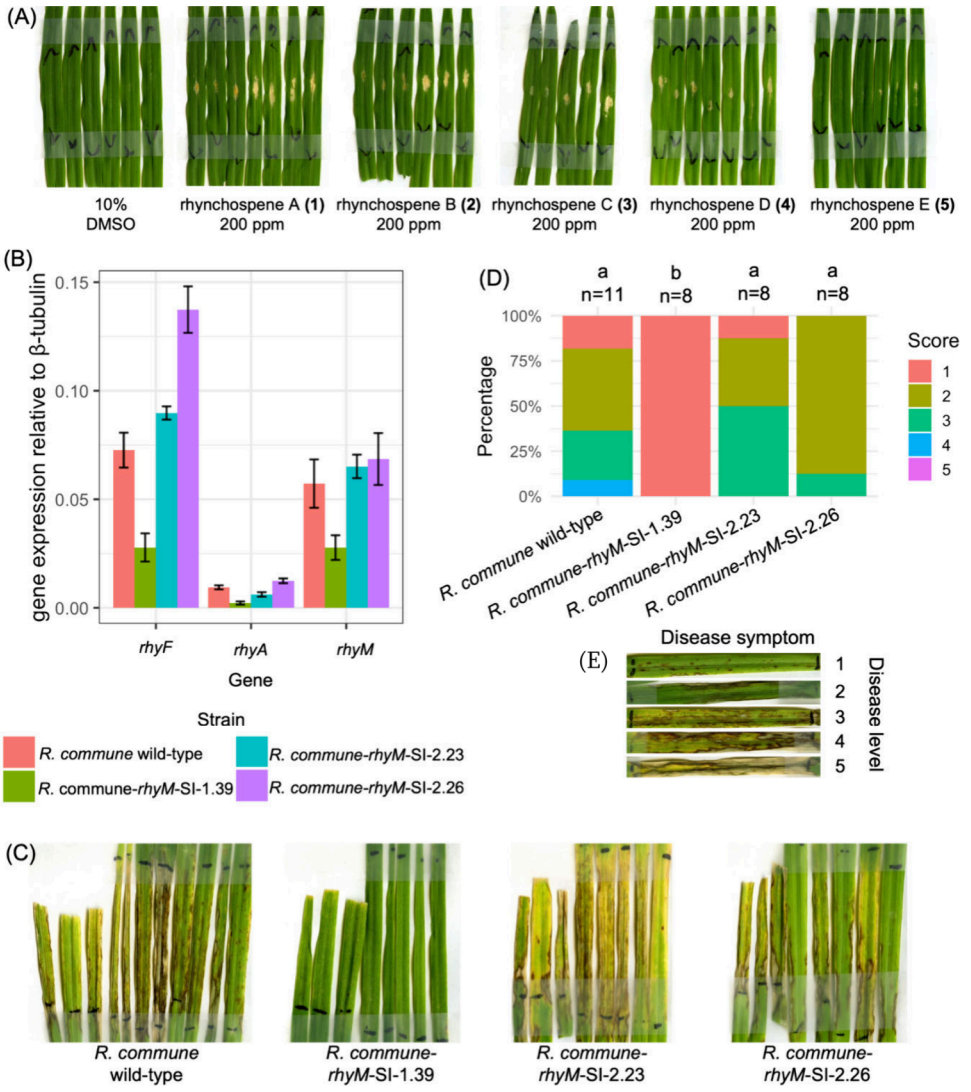

Figure 5. Toxicity of rhynchospenes in barley leaf infiltration assays and the reduced virulence of *rhyM* silencing mutant suggest the metabolites are virulence factors of *R. commune*. (A) Phytotoxicity assay of rhynchospenes A−E (**1**−**5**) at a concentration of 200 ppm infiltrated into 1st and 2nd true leaves of 2-week-old barley showed **1**−**5** induced necrosis on barley leaves. Pictures were taken at 3-dpi. (B) The 3rd leaves of barley were infected with wild-type *R. commune* WAI453 or the mutant strains *R. commune-rhyM*-SI mutants, and RNA from those infected leaves was extracted at 7-dpi to analyze the expression of *rhyA*, *rhyM*, and *rhyF* using quantitative reverse transcription PCR (qRT-PCR). Gene expression level was normalized to that for *β*-tubulin. Error bars represent the standard error of three different technical replicates. The silencing mutant *R. commune-rhyM*-SI-1.39 had a lower expression level of *rhyA*, *rhyM*, and *rhyF* compared to those in the wild-type *R. commune*. (C) Images represent the infection level of barley leaves infected with the wild-type *R. commune* or the mutant strains *R. commune-rhyM*-SI mutants taken at 12-dpi. The silencing mutant *R. commune-rhyM*-SI-1.39 strain has a lower pathogenicity level compared to the wild-type *R. commune*. (D) Infected leaves were scored based on disease severity. The number of replicates is shown on the top of each bar. One-way ANOVA with Tukey's Honest Significant Difference (HSD) test was used to test the differences between groups. The score from individual group is concluded to be significantly different from others at $P < 0.05$ if it does not share the same letter with other groups. The letter is shown above each bar. (E) The infected leaves represent each disease severity score in the fungal pathogenicity assay.

protein family shown to be involved in the biosynthesis of fungal RiPPs known as dikaritins.[29,47−49] However, more recently, DUF3328 proteins have also been shown to be involved in halogenation reactions, such as in the biosynthesis of the cyclic peptide cyclochlorotine, whereby a DUF3328 protein installs two chlorine atoms on the proline ring.[50] Hence, RhyE is likely responsible for the C-3 chlorination of **1** and **3**. The antiSMASH prediction of the BGC as encoding indole-containing SMs is likely due to the detection of the *rhyF* encoding an aromatic prenyltransferase, which is often classified as a dimethylallyl tryptophan synthase (DMATS) or indole prenyltransferase due to the functions of the original members characterized in this family. In the *rhy* cluster, RhyF most likely acts as a farnesyltransferase, which transfers the sesquiterpene moiety to the cyclopaldic acid subunit. Nonetheless, the *rhy* cluster appeared to be lacking a terpene cyclase, which is required to catalyze cyclization of the sesquiterpene to the drimane scaffold.

To gain further insight into the biosynthetic pathway to **1**−**5**, we used cblaster[51] to search the NCBI database for colocalized homologues of the *rhy* cluster genes. The search identified the complete *rhy* cluster in two closely related species, *R. agropyri* and *R. secalis*, both known as grass pathogens (Figures S10A and S10B).[4] Beyond *Rhynchospo-*

https://doi.org/10.1021/acschembio.4c00731
ACS Chem. Biol. 2025, 20, 421−431

rium, partial *rhy* clusters with the high cblaster scores (>17) were also found (Figures S10A and S10B). Notably, many species within genera *Rhynchosporium*, *Colletotrichum*, and *Diaporthe* are phytopathogens, suggesting that the *rhy* BGC and its homologues may play a role in the pathogenicity of these plant pathogens (Figures S10A and S10B). Interestingly, both the *mfm* cluster from *Annulohypoxylon moriforme* CBS 123579, and the *ocd* cluster from *Colletotrichum orchidophilum* IMI 309357, which partially overlaps with the *rhy* cluster, have been recently reported to encode drimane−phthalide hybrid metabolites.[29]

Of the 17 genes located within the *rhy* BGC, ten share 30−60% protein sequence similarity with those in the recently characterized *mfm* BGC from *Annulohypoxylon moriforme* CBS 123579, which encodes a drimane−phthalide hybrid metabolite, although the overall similarity between the two BGCs is less than 50% (Figure S10C).[29] Significantly, the matching of RhyP to MfmH (46% identity) suggests that RhyP belongs to the Pyr4-like membrane-bound terpene cyclases and is likely responsible for the formation of the drimane scaffold. Based on the predicted functions of annotated genes in the *rhy* BGC (Table S2) and the experimentally validated roles of homologous genes in the *mfm* cluster,[29] we propose a biosynthetic pathway to **1**−**5** (Figures 4 and S11). Briefly, the pathway starts with the PKS RhyA, which synthesizes 3,5-dimethylorsellinic acid (DMOA), a key precursor for various fungal meroterpenoids. Subsequent oxidation steps, catalyzed by RhyO (a cytochrome P450 monooxygenase) and RhyI (an esterase), convert DMOA into 3′-deoxy-7′-demethyl-11′-hydroxyccyclopaldic acid (intermediate I). Next, RhyK, an *O*-methyltransferase, methylates the 7′-hydroxy group of intermediate I. Subsequent modifications by RhyC (a cytochrome P450 monooxygenase) and RhyQ (a methyltransferase) lead to the production of 3′-*O*-methyl-11′-hydroxycyclopaldic acid (intermediate II). Retrobiosynthetic analysis suggests that RhyF likely acts as a reverse farnesyltransferase, which catalyzes condensation of intermediate II with the nerolidyl cation. This leads to a nerolidylated intermediate III, which is cyclized by the Pyr4-like terpene cyclase RhyP to yield intermediate IV, in which the polyketide-derived phthalide is linked to the drimanol via a C-8−C-11′ ether linkage, rather than the C-11−C-11′ ether linkage in 11′-*O*-desmethylfendlerol A/B encoded by the *mfm* cluster.[29] The successive action of either RhyJ, RhyL, or RhyN (a cytochrome P450 monooxygenase) is proposed to oxidize the C-11 alcohol to an aldehyde and then to a carboxylic acid to give **4**. Subsequently, **4** undergoes 5,6-dehydration, 5,6-epoxidation, and 3-halogenation, yielding **5**, **2** and **1**, successively. Notably, the 3-halogenation is likely catalyzed by RhyE, a DUF3328-domain-containing protein shown to be capable of catalyzing halogenation in addition to RiPP cyclization.[50] Compound **3** may be generated by the attack of water on the C-5/C-6 double bond of intermediate V (the C-3 chlorinated form of **5**), possibly by an endogenous enzyme not encoded in the *rhy* cluster.

Rhynchospenes Are Produced as Virulence Factors during Barley Leaf Infection. Given the significant upregulation of the *rhy* cluster during *R. commune* infection of barley leaves, we investigated whether the rhynchospenes are present during *in planta* growth. Barley leaves were infected with the wild-type *R. commune* strain and harvested for metabolite extraction and LC-MS analysis at the onset of necrotrophy and at the later stages of infection (see Supporting Information). Interestingly, **1**−**5** were not detected in the extracts of infected barley leaves at the onset of necrosis (6- or 8-dpi), but were detected in infected leaves at 10-dpi, where the infected leaves were heavily necrotic (Figure S12). Given the high level of expression of the *rhy* cluster at the onset of necrotrophy, it was possible that **1**−**5** were below the LC-MS detection limit at the earlier time points, due to the low biomass prior to extensive colonization of the leaves during the necrotrophy phase and that the metabolites only accumulated to a detectable level at later time points.

To validate the function of the rhynchospenes, each pure compound was infiltrated into barley leaves at the concentrations ranging from 25−800 ppm. We observed that **1**−**5** elicited varying degrees of localized necrosis around the infiltration marks at different concentrations (Figures 5A and S13, Table S4). Among these compounds, **2** exhibited the highest phytotoxicity, as evidenced by the induction of localized cell death at a concentration of 50 ppm, whereas **5** induced necrosis only at a higher concentration of 400 ppm. Moreover, **1**, **3** and **4** showed necrotic effects starting at concentrations of 100−200 ppm. These findings strongly support the notion that the rhynchospenes are phytotoxic compounds produced by *R. commune* during *in planta* growth. The upregulation of *rhy* cluster during the onset of necrotrophy suggests that the rhynchospenes play a role in the transition to necrotrophy by inducing localized plant cell death.

Having demonstrated that the cluster-specific transcription factor RhyM regulates the expression of the *rhy* BGC, which produces phytotoxic metabolites **1**−**5**, we hypothesized that RhyM could play a crucial role in the virulence of *R. commune*. Typically, gene disruption through a reverse genetic approach is employed to investigate the gene function. However, generating gene knockouts in *R. commune* is challenging due to its low rate of homologous recombination.[52] As an alternative approach, we employed gene silencing to investigate the role of RhyM in fungal virulence. The plasmid for *rhyM* silencing (158 bp of *rhyM* antisense with the *gpdA* promoter) was introduced ectopically into the *R. commune* WAI453 genome to generate the *R. commune rhyM*-SI mutants. These mutants were then subsequently used to infect the third true leaves of barley plants to assess the *rhy* BGC expression and virulence. To evaluate the effectiveness of the gene silencing construct in reducing *rhyM* expression, the expression of *rhyM* and two other *rhy* genes, *rhyA* and *rhyF*, that are controlled by RhyM, was analyzed using qRT-PCR from barley leaves infected by *R. commune* WAI453 or *R. commune rhyM*-SI mutants. In contrast to the high expression of *rhyA, rhyM*, and *rhyF* observed in the wild-type strain at 7-dpi, one of the tested mutants, *R. commune rhyM*-SI-1.39, exhibited a notable decrease in *rhyM* expression, with only 0.48-fold expression compared to that of the wild-type strain (Figure 5B), confirming the successful silencing of the *rhyM* gene. More importantly, this mutant displayed reduced expression of *rhyA* (0.23-fold) and *rhyF* (0.38-fold) compared to the wild-type strain (Figure 5B). The impact of reduced *rhy* gene expression on infection was determined by visually assessing leaves infected with either the wild-type or silenced strain at 12-dpi. Interestingly, *R. commune rhyM*-SI-1.39 exhibited a significant reduction in lesion formation compared to the wild-type strain (Figures 5C and 5D), indicating that this mutant is reduced in virulence. Collectively, these findings strongly support a positive correlation between the expression level of the *rhy*

https://doi.org/10.1021/acschembio.4c00731
ACS Chem. Biol. 2025, 20, 421−431

cluster and the induction of necrosis during barley leaf infection, underscoring the role of rhynchospenes as key virulence factors.

CONCLUSIONS

In this study, we identified the *rhy* BGC from the barley pathogen *Rhynchosporium commune* by employing a chemical ecogenomics approach. This cluster is highly upregulated at the transcriptomic level exclusively during *in planta* growth, suggesting its involvement in pathogenesis. By overexpressing the cluster-specific transcription factor RhyM—a MYB-class transcription factor that is rare in fungi—we successfully activated the production of a new group of meroterpenoids, rhynchospenes A−E (**1**−**5**), as the products of the *rhy* cluster under axenic culture. Our study is one of only a limited number of examples demonstrating the use of MYB-type transcription factor overexpression to activate conditionally silent BGCs for SM production. This approach may provide new avenues for uncovering cryptic SMs involved in environmental and host adaptations.

Rhynchospenes consist of sesquiterpene-derived drimanol and polyketide-derived phthalide moieties connected by a C-8−C-11′ ether linkage. The biosynthesis likely involves an unusual reverse farnesylation reaction catalyzed by RhyF, which warrants further investigation. The *rhy* cluster also features the recently identified class of halogenases belonging to the DUF3328 protein family. Significantly, we demonstrated that rhynchospenes induce necrosis in barley leaves, and the pathway knockdown mutant exhibited lower virulence compared to the wild-type, establishing their roles as critical virulence factors in *R. commune* pathogenesis. Our study represents the first characterization of SM BGCs from the phytopathogenic fungus *R. commune*, shedding light on the virulence mechanisms linked to *R. commune* SMs. The discovery of rhynchospenes and their roles in inducing necrosis in barley leaves advances our understanding of fungal-host interactions. These findings provide a solid foundation for future research aimed at unravelling the biosynthetic pathways to the rhynchospenes, elucidating the molecular mechanisms by which they contribute to pathogenesis, and exploring other upregulated BGCs during the *in planta* growth of *R. commune*, with potential implications for crop disease management.

MATERIALS AND METHODS

Transcription Analysis of the *rhy* Cluster in *R. commune* WAI453. The RNA-seq data set recently generated by Darma et al.[22] was used to analyze the transcription level of the *rhy* cluster *in planta* at 8-dpi and after 8 days of *in vitro* culture. In addition, the transcription level of *rhyA* was analyzed at four different time points *in planta* (3-dpi, 6-dpi, 9-dpi, and 12-dpi) using qRT-PCR (see Supporting Information).

Prediction, Annotation, and Synteny Analysis of the *rhy* Biosynthetic Gene Cluster from *R. commune* WAI453. The putative secondary metabolite biosynthetic gene clusters (BGCs) in the genome of *R. commune* WAI453 were predicted using antiSMASH fungal version 7.0.0.[21] The function of each protein encoded by the genes in the *rhy* cluster was predicted by a BLASTP search and listed in Table S2. Search of the *rhy* cluster homologues was carried out using the online program "CompArative GEne Cluster Analysis Toolbox" (CAGECAT, cagecat.bioinformatics.nl). The tool utilizes two programs: cblaster[51] that searches homologous gene clusters in the online databases and clinker[53] that generates figures from the cblaster results. CAGECAT was run with the following parameters: maximum hits 500, maximum E-value 0.01, minimum identity 30%, minimum query coverage 50%, maximum intergenic gap of the cluster 20000, minimum percentage of query genes present in cluster 50, minimum unique query hits 3, and minimum hits in clusters 3. Only gene clusters from *R. commune* sister species and from other representative genus with a score >17 were used in this analysis. The conserved functional domains present in the PKS RhyA were analyzed using the synthaser[23] program (https://github.com/gamcil/synthaser) with the default settings.

Construction of the *R. commune rhyM*-OE and *R. commune rhyM*-SI Mutant Strains. A plasmid (*rhyM*-OE) containing the transcription factor gene *rhyM* controlled by the *gpdA* promoter and a hygromycin resistance gene (*hph*) marker was used to construct the *R. commune rhyM*-OE strain. Whereas the *rhyM*-SI plasmid containing a 158 bp from the third exon of *rhyM* gene in the reverse complement order (antisense) controlled by *gpdA* promoter and a glufosinate resistance gene (*bar*) marker was used to construct the *R. commune rhyM*-SI silencing mutant strain. Transformation of *R. commune* with the two plasmids were achieved using *Agrobacterium tumefaciens*-mediated transformation (ATMT). Detailed description of the plasmid construction, transformation, and screening is included in the Supporting Information.

Metabolite Analysis of the *R. commune* Wild-Type and *rhyM*-OE Strains. The *R. commune* wild-type and *rhyM*-OE strains were inoculated in two culture media, including lima bean broth (20 °C, 180 rpm, 8 days) and rice solid media (RT, static, 60 days). After cultivation, the fungal biomasses together with culture media were extracted with EtOAc followed by drying of the organic phase *in vacuo* to yield crude extracts. Analytes of the extracts (5 mg mL^{-1}) were prepared in MeOH and analyzed by LCMS using standard gradient elution condition (Kinetex C18 column; 100 Å; 100 × 2.1 mm; 0.7 mL/min gradient elution from 95% H_2O/MeCN to 100% MeCN with 0.1% formic acid over 10 min). The metabolites exclusively produced by the *R. commune rhyM*-OE strain were differentiated by a comparison of the HPLC and the total ion current (TIC) chromatograms to those of the *R. commune* wild-type strain.

Purification and Structure Elucidation of Rhynchospenes A−E (1−5). To obtain adequate amounts of the activated metabolites for structure elucidation and bioassays, the *R. commune rhyM*-OE strain was cultivated on rice solid media, followed by ethyl acetate extraction and purification using preparative HPLC (see Supporting Information). Each purified compound was dried *in vacuo* and redissolved in 500 μL of $CDCl_3$ or CD_3OD for nuclear magnetic resonance (NMR) analysis. The ^1H, ^{13}C, HSQC, HMBC, ^1H−^1H COSY, and ^1H−^1H NOESY spectra were acquired on a Bruker Avance III HD 600 MHz spectrometer with a BBFO probe controlled by TopSpin 3.6.2 software. All spectra were referenced to residual ^1H or ^{13}C signals in $CDCl_3$ (δ_H 7.26 and δ_C 77.16) or CD_3OD (δ_H 3.31 and δ_C 49.0). Detailed characterization of each compound is included in Supporting Information.

X-ray Crystallographic Analysis of Rhynchospenes A (1) and D (4). Crystallographic data for **1** and **4** were collected on a HyPix diffractometer by using CuKα radiation. The structures were solved using the ShelXT program with Olex2 as the graphical interface and Intrinsic Phasing solution method. The models were refined with the 2018/3 version of ShelXL, employing Least Squares minimization.[54−56] H atom positions were calculated geometrically and refined by using the riding model.

Barley Leaves Infiltration Assay for Rhynchospenes A−E (1−5). Different concentrations (25, 50, 100, 200, 400, and 800 ppm) of rhynchospenes in 10% aqueous DMSO were infiltrated into the first and second true leaves of two-week-old seedlings of barley cv. Atlas 46. A solution of 10% aqueous DMSO was used as the negative control. Subsequently, the barley plants were moved to a growth chamber for additional incubation under normal barley growth conditions for another 3 days. The infiltrated leaves were then harvested and the phytotoxic activity of the rhynchospenes was scored based on the necrosis area in the infiltrated leaves.

https://doi.org/10.1021/acschembio.4c00731
ACS Chem. Biol. 2025, 20, 421−431

■ ASSOCIATED CONTENT

Supporting Information

The Supporting Information is available free of charge at https://pubs.acs.org/doi/10.1021/acschembio.4c00731.

Additional experimental details; information on plasmids and primers; bioinformatics analysis including *Rhy* BGC composition and synteny analysis; other biological characterization data; chemical and structural characterization of rhynchospenes A−E, including 1D and 2D NMR data, X-ray crystallographic data, UV−vis, ECD, HRMS spectra (PDF)

Predicted BGCs of *R. commune* WAI453 and their Log2 Fold Change value from the transcriptomics data listed in Data File S1 (XLSX)

■ AUTHOR INFORMATION

Corresponding Authors

Yit-Heng Chooi − *School of Molecular Sciences, The University of Western Australia, Perth, WA 6009, Australia;* orcid.org/0000-0001-7719-7524; Email: yitheng.chooi@uwa.edu.au

Peter S. Solomon − *Research School of Biology, The Australian National University, Canberra, ACT 2601, Australia*; Email: peter.solomon@anu.edu.au

Zhuo Shang − *School of Molecular Sciences, The University of Western Australia, Perth, WA 6009, Australia; School of Pharmaceutical Sciences, Cheeloo College of Medicine, Shandong University, Jinan, Shandong 250012, China*; Email: zshang@email.sdu.edu.cn

Authors

Reynaldi Darma − *Research School of Biology, The Australian National University, Canberra, ACT 2601, Australia; Department of Protecting Crops and the Environment, Rothamsted Research, Harpenden, Hertfordshire AL5 2JQ, U.K.*

Joe Bracegirdle − *School of Molecular Sciences, The University of Western Australia, Perth, WA 6009, Australia*

Stephen Moggach − *School of Molecular Sciences, The University of Western Australia, Perth, WA 6009, Australia;* orcid.org/0000-0001-5339-7070

Megan C. McDonald − *Research School of Biology, The Australian National University, Canberra, ACT 2601, Australia; School of Biosciences, Institute of Microbiology and Infection, University of Birmingham, Birmingham B15 2TT, U.K.*

Andrew M. Piggott − *School of Natural Sciences, Macquarie University, Sydney, NSW 2109, Australia;* orcid.org/0000-0002-5308-5314

Complete contact information is available at: https://pubs.acs.org/10.1021/acschembio.4c00731

Author Contributions

¶R.D. and Z.S. contributed equally to this work.

Notes

The authors declare no competing financial interest.

■ ACKNOWLEDGMENTS

This research was funded by the Australian Research Council (DP200101880 to Y−H.C. and P.S. and FT160100233 to Y−H.C.) and the National Natural Science Foundation of China (U23A20107 to Z.S.). R.D. was supported by the Australian National University scholarships and The British Society for Plant Pathology (BSPP) COVID-19 support.

■ REFERENCES

(1) Brown, J. S. Pathogenic Variation Among Isolates of *Rhynchosporium secalis* from Cultivated Barley Growing in Victoria, Australia. *Euphytica* **1985**, *34*, 129−133.

(2) *Barley Disease Management Guide*; Agriculture and Horticulture Development Board Cereals & Oilseeds, 2016.

(3) Davis, J. J. Notes on Parasitic Fungi in Wisconsin-V. *Trans. Wis. Acad. Sci. Arts Lett.* **1919**, *19*, 690−704.

(4) Zaffarano, P. L.; McDonald, B. A.; Linde, C. C. Two New Species of *Rhynchosporium*. *Mycologia* **2011**, *103*, 195−202.

(5) Avrova, A.; Knogge, W. *Rhynchosporium commune*: A Persistent Threat to Barley Cultivation. *Mol. Plant Pathol.* **2012**, *13*, 986−997.

(6) Zhan, J.; Fitt, B. D. L.; Pinnschmidt, H. O.; Oxley, S. J. P.; Newton, A. C. Resistance, Epidemiology and Sustainable Management of *Rhynchosporium secalis* Populations on Barley. *Plant Pathol.* **2008**, *57*, 1−14.

(7) Skoropad, W. P. Seed and Seedling Infection of Barley by *Rhynchosporium secalis*. *Phytopathology* **1959**, *49*, 623−626.

(8) Chooi, Y. H.; Zhang, G.; Hu, J.; Muria-Gonzalez, M. J.; Tran, P. N.; Pettitt, A.; Maier, A. G.; Barrow, R. A.; Solomon, P. S. Functional Genomics-Guided Discovery of a Light-Activated Phytotoxin in the Wheat Pathogen *Parastagonospora nodorum* Via Pathway Activation. *Environ. Microbiol.* **2017**, *19*, 1975−1986.

(9) Li, H.; Wei, H.; Hu, J.; Lacey, E.; Sobolev, A. N.; Stubbs, K. A.; Solomon, P. S.; Chooi, Y. H. Genomics-Driven Discovery of Phytotoxic Cytochalasans Involved in the Virulence of the Wheat Pathogen *Parastagonospora nodorum*. *ACS Chem. Biol.* **2020**, *15*, 226−233.

(10) Li, H.; Hu, J.; Wei, H.; Solomon, P. S.; Vuong, D.; Lacey, E.; Stubbs, K. A.; Piggott, A. M.; Chooi, Y. H. Chemical Ecogenomics-Guided Discovery of Phytotoxic Alpha-Pyrones from the Fungal Wheat Pathogen *Parastagonospora nodorum*. *Org. Lett.* **2018**, *20*, 6148−6152.

(11) Ayesu-Offei, E. N.; Clare, B. G. Symptoms of Scald Disease Induced by Toxic Metabolites of *Rhynchosporium secalis*. *Aust. J. Biol. Sci.* **1971**, *24*, 169−174.

(12) Auriol, P.; Strobel, G.; Beltran, J. P.; Gray, G. Rhynchosporoside, a Host-Selective Toxin Produced by *Rhynchosporium secalis*, the Causal Agent of Scald Disease of Barley. *Proc. Natl. Acad. Sci. U. S. A.* **1978**, *75*, 4339−4343.

(13) Caldwell, R. M. Rhynchosporium Scald of Barley, Rye, and Other Grasses. *J. Agric. Res.* **1937**, *55*, 175−198.

(14) Ichihara, A.; Hashimoto, M.; Hirai, T.; Takeda, I.; Sasamura, Y.; Sakamura, S.; Sato, R.; Tajimi, A. Structure, Synthesis, and Stereochemistry of (+)-Orthosporin, a Phytotoxic Metabolite of *Rhynchosporium orthosporum*. *Chem. Lett.* **1989**, *18*, 1495−1498.

(15) Hallock, Y. F.; Clardy, J.; Kenfield, D. S.; Strobel, G. De-O-Methyldiaporthin, a Phytotoxin from *Drechslera siccans*. *Phytochemistry* **1988**, *27*, 3123−3125.

(16) Harris, J. P.; Mantle, P. G. Biosynthesis of Diaporthin and Orthosporin by *Aspergillus ochraceus*. *Phytochemistry* **2001**, *57*, 165−169.

(17) Wiemann, P.; Keller, N. P. Strategies for Mining Fungal Natural Products. *J. Ind. Microbiol. Biotechnol.* **2014**, *41*, 301−313.

(18) Kessler, S. C.; Zhang, X.; McDonald, M. C.; Gilchrist, C. L. M.; Lin, Z.; Rightmyer, A.; Solomon, P. S.; Turgeon, B. G.; Chooi, Y. H. Victorin, the Host-Selective Cyclic Peptide Toxin From the Oat Pathogen *Cochliobolus victoriae*, Is Ribosomally Encoded. *Proc. Natl. Acad. Sci. U. S. A.* **2020**, *117*, 24243−24250.

(19) Penselin, D.; Munsterkotter, M.; Kirsten, S.; Felder, M.; Taudien, S.; Platzer, M.; Ashelford, K.; Paskiewicz, K. H.; Harrison, R. J.; Hughes, D. J.; et al. Comparative Genomics to Explore Phylogenetic Relationship, Cryptic Sexual Potential and Host Specificity of *Rhynchosporium* Species on Grasses. *BMC Genomics* **2016**, *17*, 953.

(20) Chooi, Y. H.; Solomon, P. S. A Chemical Ecogenomics Approach to Understand the Roles of Secondary Metabolites in Fungal Cereal Pathogens. *Front. Microbiol.* **2014**, *5*, 640.
(21) Blin, K.; Shaw, S.; Augustijn, H. E; Reitz, Z. L; Biermann, F.; Alanjary, M.; Fetter, A.; Terlouw, B. R; Metcalf, W. W; Helfrich, E. J N; van Wezel, G. P; Medema, M. H; Weber, T.; et al. AntiSMASH 7.0: New and Improved Predictions for Detection, Regulation, Chemical Structures and Visualisation. *Nucleic Acids Res.* **2023**, *51*, W46−W50.
(22) Darma, R.; Yu, D. S.; Outram, M. A.; Sung, Y. C.; Hill, E. H.; Croll, D.; Williams, S. J.; Ovenden, B.; Milgate, A.; Solomon, P. S.; McDonald, M. C. Revisiting the Evolution and Function of NIP2 Paralogs in the *Rhynchosporium* spp. Complex. *bioRxiv* 2024. DOI: 10.1101/2024.10.15.618441.
(23) Gilchrist, C. L. M.; Chooi, Y. H. Synthaser: A CD-Search Enabled Python Toolkit for Analysing Domain Architecture of Fungal Secondary Metabolite Megasynth(et)ases. *Fungal Biol. Biotechnol.* **2021**, *8*, 13.
(24) Wang, J.; Chitsaz, F.; Derbyshire, M. K.; Gonzales, N. R.; Gwadz, M.; Lu, S.; Marchler, G. H.; Song, J. S.; Thanki, N.; Yamashita, R. A.; Yang, M.; Zhang, D.; Zheng, C.; Lanczycki, C. J.; Marchler-Bauer, A. The Conserved Domain Database in 2023. *Nucleic Acids Res.* **2023**, *51*, D384−D388.
(25) Mirdita, M.; Schütze, K.; Moriwaki, Y.; Heo, L.; Ovchinnikov, S.; Steinegger, M. ColabFold: Making Protein Folding Accessible to All. *Nat. Methods* **2022**, *19*, 679−682.
(26) van Kempen, M.; Kim, S. S.; Tumescheit, C.; Mirdita, M.; Lee, J.; Gilchrist, C. L. M.; Soding, J.; Steinegger, M. Fast and Accurate Protein Structure Search with Foldseek. *Nat. Biotechnol.* **2024**, *42*, 243−246.
(27) Kelley, L. A.; Mezulis, S.; Yates, C. M.; Wass, M. N.; Sternberg, M. J. The Phyre2 Web Portal for Protein Modeling, Prediction and Analysis. *Nat. Protoc.* **2015**, *10*, 845−858.
(28) Winter, J. M.; Cascio, D.; Dietrich, D.; Sato, M.; Watanabe, K.; Sawaya, M. R.; Vederas, J. C.; Tang, Y. Biochemical and Structural Basis for Controlling Chemical Modularity in Fungal Polyketide Biosynthesis. *J. Am. Chem. Soc.* **2015**, *137*, 9885−9893.
(29) Yan, D.; Matsuda, Y. Global Genome Mining-Driven Discovery of an Unusual Biosynthetic Logic for Fungal Polyketide-Terpenoid Hybrids. *Chem. Sci.* **2024**, *15*, 3011−3017.
(30) Rojas-Aedo, J. F.; Gil-Duran, C.; Del-Cid, A.; Valdes, N.; Alamos, P.; Vaca, I.; Garcia-Rico, R. O.; Levican, G.; Tello, M.; Chavez, R. The Biosynthetic Gene Cluster for Andrastin A in *Penicillium roqueforti*. *Front. Microbiol.* **2017**, *8*, 813.
(31) van den Berg, M. A.; Albang, R.; Albermann, K.; Badger, J. H.; Daran, J. M.; Driessen, A. J.; Garcia-Estrada, C.; Fedorova, N. D.; Harris, D. M.; Heijne, W. H.; Joardar, V.; Kiel, J. A.; Kovalchuk, A.; Martín, J. F.; Nierman, W. C.; Nijland, J. G.; Pronk, J. T.; Roubos, J. A.; van der Klei, I. J.; van Peij, N. N.; Veenhuis, M.; von Döhren, H.; Wagner, C.; Wortman, J.; Bovenberg, R. A. Genome Sequencing and Analysis of the Filamentous Fungus *Penicillium chrysogenum*. *Nat. Biotechnol.* **2008**, *26*, 1161−1168.
(32) Tsushima, A.; Gan, P.; Kumakura, N.; Narusaka, M.; Takano, Y.; Narusaka, Y.; Shirasu, K. Genomic Plasticity Mediated by Transposable Elements in the Plant Pathogenic Fungus *Colletotrichum higginsianum*. *Genome Biol. Evol.* **2019**, *11*, 1487−1500.
(33) Matsuda, Y.; Wakimoto, T.; Mori, T.; Awakawa, T.; Abe, I. Complete Biosynthetic Pathway of Anditomin: Nature's Sophisticated Synthetic Route to a Complex Fungal Meroterpenoid. *J. Am. Chem. Soc.* **2014**, *136*, 15326−15336.
(34) Del-Cid, A.; Gil-Duran, C.; Vaca, I.; Rojas-Aedo, J. F.; Garcia-Rico, R. O.; Levican, G.; Chavez, R. Identification and Functional Analysis of the Mycophenolic Acid Gene Cluster of *Penicillium roqueforti*. *PLoS One* **2016**, *11*, e0147047.
(35) Tao, H.; Abe, I. Enzymology and Biosynthesis of the Orsellinic Acid Derived Medicinal Meroterpenoids. *Curr. Opin. Biotechnol.* **2021**, *69*, 52−59.
(36) Pfütze, S.; Charria-Girón, E.; Schulzke, E.; Toshe, R.; Khonsanit, A.; Franke, R.; Surup, F.; Brönstrup, M.; Stadler, M. Depicting the Chemical Diversity of Bioactive Meroterpenoids Produced by the Largest Organism on Earth. *Angew. Chem., Int. Ed. Engl.* **2024**, *63*, e202318505.
(37) Darma, R.; Lutz, A.; Elliott, C. E.; Idnurm, A. Identification of a Gene Cluster for the Synthesis of the Plant Hormone Abscisic Acid in the Plant Pathogen *Leptosphaeria maculans*. *Fungal Genet. Biol.* **2019**, *130*, 62−71.
(38) Shelest, E. Transcription Factors in Fungi. *FEMS Microbiol. Lett.* **2008**, *286*, 145−151.
(39) Shelest, E. Transcription Factors in Fungi: TFome Dynamics, Three Major Families, and Dual-Specificity TFs. *Front. Genet.* **2017**, *8*, 53.
(40) Verma, S.; Gazara, R. K.; Verma, P. K. Transcription Factor Repertoire of Necrotrophic Fungal Phytopathogen *Ascochyta rabiei*: Predominance of MYB Transcription Factors as Potential Regulators of Secretome. *Front. Plant Sci.* **2017**, *8*, 1037.
(41) Ambawat, S.; Sharma, P.; Yadav, N. R.; Yadav, R. C. MYB Transcription Factor Genes as Regulators for Plant Responses: An Overview. *Physiol. Mol. Biol. Plants* **2013**, *19*, 307−321.
(42) Lee, S.; Völz, R.; Song, H.; Harris, W.; Lee, Y. H. Characterization of the MYB Genes Reveals Insights Into Their Evolutionary Conservation, Structural Diversity, and Functional Roles in *Magnaporthe oryzae*. *Front. Microbiol.* **2021**, *12*, 721530.
(43) Reyes-Fernández, E. Z.; Shi, Y. M.; Grün, P.; Bode, H. B.; Bölker, M. An Unconventional Melanin Biosynthesis Pathway in *Ustilago maydis*. *Appl. Environ. Microbiol.* **2021**, *87*, e01510-20.
(44) Li, Y.; Zheng, X. X.; Pei, M. T.; Chen, M. T.; Zhang, S. N.; Liang, C. Y.; Gao, L. Y.; Huang, P.; Olsson, S. Functional Analysis of MoMyb13, a Myb Transcription Factor Involved in Regulating Growth, Conidiation, Hydrophobicity, and Pathogenicity of *Magnaporthe oryzae*. *Agronomy (Basel)* **2024**, *14*, 251.
(45) Liu, B.; Han, J.; Zhang, H.; Li, Y.; An, Y.; Ji, S.; Liu, Z. The Regulatory Pathway of Transcription Factor MYB36 from *Trichoderma asperellum* Tas653 Resistant to Poplar Leaf Blight Pathogen *Alternaria alternata* Aal004. *Microbiol. Res.* **2024**, *282*, 127637.
(46) Hemberger, Y.; Xu, J.; Wray, V.; Proksch, P.; Wu, J.; Bringmann, G. Pestalotiopens A and B: Stereochemically Challenging Flexible Sesquiterpene-Cyclopaldic Acid Hybrids from *Pestalotiopsis* sp. *Chemistry* **2013**, *19*, 15556−15564.
(47) Ding, W.; Liu, W. Q.; Jia, Y.; Li, Y.; van der Donk, W. A.; Zhang, Q. Biosynthetic Investigation of Phomopsins Reveals a Widespread Pathway for Ribosomal Natural Products in Ascomycetes. *Proc. Natl. Acad. Sci. U. S. A.* **2016**, *113*, 3521−3526.
(48) Ye, Y.; Minami, A.; Igarashi, Y.; Izumikawa, M.; Umemura, M.; Nagano, N.; Machida, M.; Kawahara, T.; Shin-ya, K.; Gomi, K.; Oikawa, H. Unveiling the Biosynthetic Pathway of the Ribosomally Synthesized and Post-translationally Modified Peptide Ustiloxin B in Filamentous Fungi. *Angew. Chem., Int. Ed.* **2016**, *55*, 8072−8075.
(49) Kessler, S. C.; Chooi, Y. H. Out for a RIPP: Challenges and Advances in Genome Mining of Ribosomal Peptides from Fungi. *Nat. Prod. Rep.* **2022**, *39*, 222−230.
(50) Jiang, Y.; Ozaki, T.; Liu, C.; Igarashi, Y.; Ye, Y.; Tang, S.; Ye, T.; Maruyama, J. I.; Minami, A.; Oikawa, H. Biosynthesis of Cyclochlorotine: Identification of the Genes Involved in Oxidative Transformations and Intramolecular O,N-Transacylation. *Org. Lett.* **2021**, *23*, 2616−2620.
(51) Gilchrist, C. L. M.; Booth, T. J.; van Wersch, B.; van Grieken, L.; Medema, M. H.; Chooi, Y. H. Cblaster: A Remote Search Tool for Rapid Identification and Visualization of Homologous Gene Clusters. *Bioinform. Adv.* **2021**, *1*, vbab016.
(52) Kirsten, S.; Navarro-Quezada, A.; Penselin, D.; Wenzel, C.; Matern, A.; Leitner, A.; Baum, T.; Seiffert, U.; Knogge, W. Necrosis-Inducing Proteins of *Rhynchosporium commune*, Effectors in Quantitative Disease Resistance. *Mol. Plant-Microbe Interact.* **2012**, *25*, 1314−1325.
(53) Gilchrist, C. L. M.; Chooi, Y. H. Clinker & Clustermap.js: Automatic Generation of Gene Cluster Comparison Figures. *Bioinformatics* **2021**, *37*, 2473−2475.

https://doi.org/10.1021/acschembio.4c00731
ACS Chem. Biol. 2025, 20, 421−431

(54) Sheldrick, G. M. Crystal structure refinement with SHELXL. *Acta Crystallogr. Sect. C: Struct. Chem.* **2015**, *71*, 3−8.
(55) Sheldrick, G. M. SHELXT-Integrated Space-Group and Crystal-Structure Determination. *Acta Crystallogr. A: Found. Adv.* **2015**, *71*, 3−8.
(56) Dolomanov, O. V.; Bourhis, L. J.; Gildea, R. J.; Howard, J. A. K.; Puschmann, H. OLEX2: A Complete Structure Solution, Refinement and Analysis Program. *J. Appl. Crystallogr.* **2009**, *42*, 339−341.

https://doi.org/10.1021/acschembio.4c00731
ACS Chem. Biol. 2025, 20, 421−431